New Method for Multiple-mode Shunt Damping of Structural Vibration using a Single Piezoelectric Transducer

S. Behrens*, A.J. Fleming, S.O.R. Moheimani.
Department of Electrical and Computer Engineering
The University of Newcastle, Australia

ABSTRACT

A new multi-mode semi-active shunt technique for controlling vibration in piezoelectric laminated structures is proposed in this paper. The effect of the "negative capacitor" controller is studied theoretically and then validated experimentally on a piezoelectric laminated simply-supported beam. The negative capacitor controller is similar in nature to passive shunt damping techniques, as a single piezoelectric transducer is used to dampen multiple modes. While achieving comparable performance to that of the purely piezoelectric passive shunt schemes, the negative capacitor controller has a number of advantages. It is simpler to implement, less sensitive to environmental variations, and can act as a multiple mode and broadband vibration controller.

Experimental resonant amplitudes for the piezoelectric laminated simply-supported beam 1st, 2nd, 3rd, 4th and 5th modes were successfully reduced by 6.1, 16.3, 15.2, 11.7 and 10.2dB.

Keywords: vibration suppression, semi-active shunt, passive damping, multiple modes, broadband.

1. INTRODUCTION

A passive vibration shunt damper[1,2,3,4] acts to minimize structural vibration at a particular frequency, associated with a lightly damped structural vibration mode. These frequencies are rarely stationary in real applications, i.e. changes in climactic conditions may shift resonant frequencies. Some damping is usually added to ensure effectiveness over a range of frequencies. Maximum amplitude reduction, is achieved only if the shunt absorber is lightly damped and precisely tuned to the required frequency of concern. Thus, a semi-active (passive-active) vibration absorber should perform better than a passive shunt damper, and could be made much simpler.

There are many different types of semi-active vibration controller schemes. One of these schemes involves modifying the effective stiffness of the piezoelectric element, by switch damping[5,6,7,8,9] . Switch damping involves switching the piezoelectric actuator element between high (open-circuit) and low (short-circuit) stiffness states. These techniques are broadband and passive, but the amplitude reduction performance is limited.

Another type of semi-active vibration controller is the active-passive hybrid piezoelectric network (APPN), which involves using a passive shunt damping network conjunction with an appropriate broadband active controller (e.g. a simple $R-L$ passive shunt with a LQG active controller[10,11,12]). This method is claimed to be more effective than a system with separated active and passive control schemes[10,11,12] .

This paper will attempt to develop a new technique for semi-active (passive-active) control. The "negative capacitor" controller is studied theoretically and then validated experimentally. The negative capacitor controller is similar in nature to passive shunt damping techniques; a single piezoelectric transducer is used, but is capable of damping multiple modes.

2. PIEZOELECTRIC MODEL

Piezoelectric devices have shown promising applications in active, semi-active, and passive vibration control. Piezoelectric materials convert mechanical strains into electrical energy and vice versa. This characteristic can be exploited, allowing them to be used as both sensors and actuators.

Piezoelectric crystals have a three-dimensional structure, i.e. crystal deformation occurs in 3 dimensions. Practical mechanical uses only require the effect in one or two dimensions, this can be approximated by manufacturing piezoelectric patches with large length and width to thickness ratios.

* Corresponding author:- Email: sbehrens@ecemail.newcastle.edu.au; Phone: +61 2 4921 7223

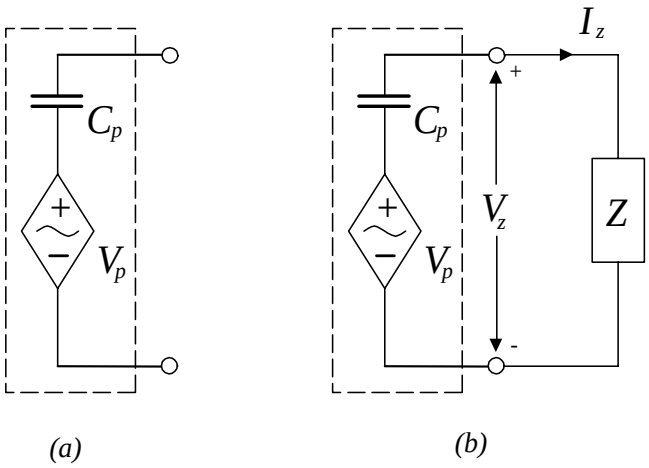

Figure 1. (a) Series equivalent model for piezoelectric shunt layer; and (b) schematic of piezoelectric shunting layer with a shunting impedance Z present.

Piezoelectric transducers behave electrically like a capacitor C_p and mechanically like a stiff spring[13] . It is common practice to model the piezoelectric element as a capacitor C_p in series with a strain dependent voltage source V_p [14,15] as shown in Figure 1 (a).

3. MODELING THE COMPOUND SYSTEM

In this section we will sketch how the dynamics of a simply-supported piezoelectric laminate beam as illustrated in Figure 2 can be derived. Two piezoelectric patches are bonded to the structure using a strong adhesive material. One piezoelectric patch will be used as an actuator to generate a disturbance and the other as a shunting layer. The subscripts "a", "b" and "s" correspond respectively to the actuating piezoelectric layer, the beam, and the shunting piezoelectric layer.

3.1. Structural Dynamics of a Simply Supported Beam

When modeling the dynamics of a structure, it is common practice to derive the transfer function between the displacement at any point along the beam and the actuator voltage, i.e., $Y(x,s)/V_a(s)$, and also the transfer function between the shunting piezoelectric voltage and the actuator voltage $V_s(s)/V_a(s)$.

The elastic deflection of a simply supported beam is described by the one dimensional Bernoulli-Euler beam equation which has been modified[16] as shown below:

$$\frac{\partial^2}{\partial x^2}\left[E_b I_b \frac{\partial^2 y(x,t)}{\partial x^2} - C_a v_a(x,t)\right] + \rho_b A_b \frac{\partial^2 y(x,t)}{\partial t^2} = 0 \tag{1}$$

where E_b, I_b, A_b and ρ_b represent the Young's modulus, moment of inertia, cross-sectional area and linear mass density of the beam respectively. The additional term is due to the moment applied to the neutral axis of the beam by the actuator piezoelectric layer, i.e., $M_a = C_a v_a(x,t)$ where C_a is a constant dependent on the actuator properties[17] . It is assumed that each piezoelectric patch is very thin and that the beam deflects only in the y axis. Simply supported boundary conditions imply $y(0,t) = y(L,t) = 0$ and $E_b I_b \frac{\partial y(0,t)}{\partial x} = E_b I_b \frac{\partial y(L,t)}{\partial x} = 0$.

By using the *modal analysis technique*[18] the position function $y(x,t)$, can be expanded as an infinite series of the form $y(x,t) = \sum_{i=1}^{\infty} \phi_i(x) q_i(t)$, where $\phi_i(x)$ are the normalized mode shapes given by $\phi_i(x) = \sqrt{\frac{2}{\rho_b A_b L}} \sin\left(\frac{i\pi x}{L}\right)$[18] , and $q_i(t)$ are the modal displacements[16] .

To formulate the dynamical response of the system, the Lagrange equations[18] are used to find the differential equation corresponding to each mode.

$$\ddot{q}_i(t) + \omega_i^2 q_i(t) = C_a[\phi_i'(x_1) - \phi_i'(x_2)] v_a(t) \tag{2}$$

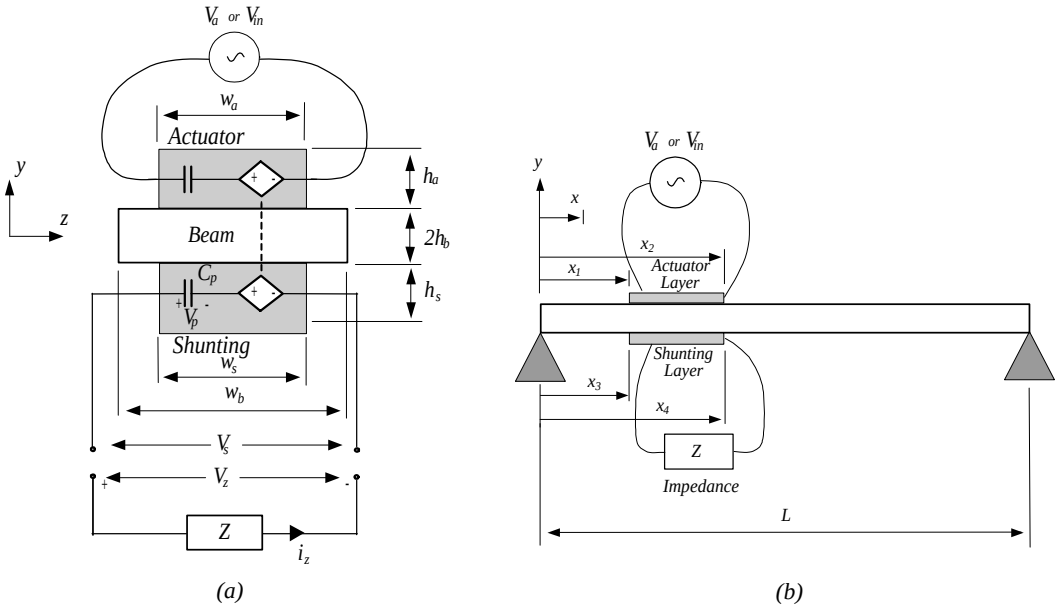

Figure 2. (a) Cross-section of the beam with piezoelectric laminates present; and (b) the piezoelectric laminated simply-supported beam.

The piezoelectric shunt sensor voltage can be described by $v_s(t) = C_s \left.\frac{\partial y(x,t)}{\partial x}\right|_{x_3}^{x_4}$ where C_s is the piezoelectric constant[16] . In the sequel we will use the notation $(\bullet)'$, $(\dot{\bullet})$ to represent the derivatives with respect to the spatial variable x, and time t, respectively. The resonant frequencies ω_i are given by $\omega_i = \left(\frac{i\pi}{L}\right)^2 \sqrt{\frac{E_b I_b}{\rho_b A_b}}$.

The dynamic response is found by taking the Laplace transform of the above equation and substituting $Y_i(x,s) = \phi_i(x)q_i(s)$.

$$G_{yv}(x,s) \triangleq \frac{Y(x,s)}{V_a(s)} = \sum_{i=1}^{\infty} \frac{C_a[\phi_i'(x_1) - \phi_i'(x_2)]\phi_i(x)}{s^2 + 2\zeta_i w_i s + w_i^2}. \tag{3}$$

The above equation describes the elastic deflection of the entire flexible beam due to a voltage applied to the piezoelectric actuator. Note that the additional terms $2\zeta_i w_i s$, are added to compensate for structural damping and are usually found experimentally. The shunting layer voltage can be expressed as $v_s(t) = C_s \sum_{i=1}^{\infty} q_i(t)(\phi_i'(x_3) - \phi_i'(x_4))$. By taking the Laplace transform, the transfer function from the actuator to shunt voltage is found to be[17] ,

$$G_{vv}(s) \triangleq \frac{V_s(s)}{V_a(s)} = \sum_{i=1}^{\infty} \frac{C_s C_a[\phi_i'(x_1) - \phi_i'(x_2)][\phi_i'(x_3) - \phi_i'(x_4)]}{s^2 + 2\zeta_i w_i s + w_i^2}. \tag{4}$$

3.2. Experimental tested: Simply Supported Beam

The experimental beam is a uniform aluminum bar with rectangular cross section and experimentally pinned boundary conditions at both ends. A pair of piezoelectric ceramic patches (PIC151) are attached symmetrically to either side of the beam surface. One patch is used as an actuator and the other as a shunting layer. Experimental beam and piezoelectric parameters are summarized in Table 1.

The displacement and voltage frequency responses are measured using a Polytec Laser Scanning Vibrometer (PSV-300) and a Hewlett Packard spectrum analyzer (35670A). In both cases a swept sine excitation is applied to the actuator piezoelectric patch. The frequency response of the experimental system and identified model is shown in Figure 3. It is observed that the identified model is a good representation of the true system over the bandwidth of interest.

Beam Parameters	
Length, L	$0.6\ m$
Width, w_b	$0.05\ m$
Thickness, h_b	$0.003\ m$
Youngs Modulus, E_b	$65 \times 10^9\ N/m^2$
Density, ρ_b	$2650\ kg/m^2$

PIC151 Parameters	
Length	$0.070\ m$
Charge Constant, d_{31}	$-210 \times 10^{-12}\ m/V$
Voltage Constant, g_{31}	$-11.5 \times 10^{-3}\ Vm/N$
Coupling Coefficient, k_{31}	0.340
Capacitance, C_p	$0.105\ \mu F$
Width, $w_s\ w_a$	$0.025\ m$
Thickness, $h_s\ h_a$	$0.25 \times 10^{-3}\ m$
Youngs Modulus, $E_s\ E_a$	$63 \times 10^9\ N/m^2$

Table 1. Parameters of the simply-supported piezoelectric laminated beam.

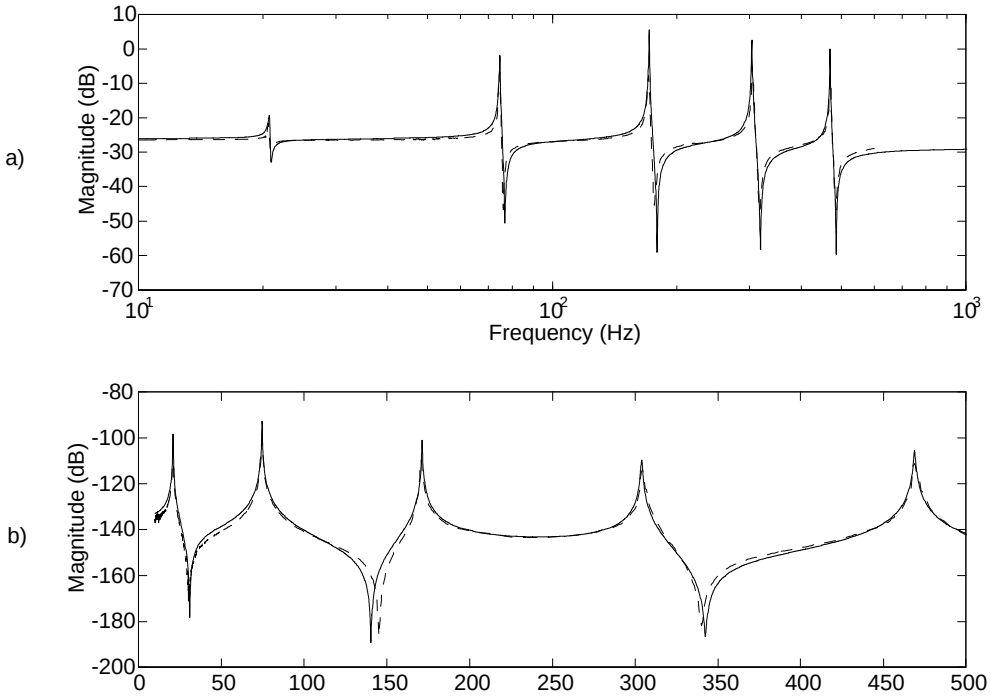

Figure 3. Frequency response of a) $\left|\frac{V_s(s)}{V_a(s)}\right|$, b) $\left|\frac{Y(0.170,s)}{V_a(s)}\right|$. Experimental ($\cdots$) and modeled results (—).

4. MODELING THE COMPOSITE SYSTEM IN TRANSFER FUNCTION FORM

Consider Figures 1 (b) and 2, where a piezoelectric patch is shunted by an impedance Z. Hence, the current-voltage relationship of the impedance can be represented in Laplace domain as

$$V_z(s) = I_z(s)Z(s) \tag{5}$$

where V_z is the voltage across the impedance and I_z is the current flowing through the impedance Z. Using Kirchhoff's voltage law the circuit shown in Figure 1 (b), we obtain $V_z(s)$ as

$$V_z(s) = V_p(s) - \frac{1}{C_p s} I_z(s) \tag{6}$$

where V_p is the voltage induced from the electromechanical coupling effect[15] and C_p represents capacitance of the shunting layer. Using (5) and (6) we obtain

$$V_z(s) = \frac{Z(s)}{\frac{1}{C_p s} + Z(s)} V_p(s) \tag{7}$$

or equivalently

$$V_z(s) = \frac{C_p s Z(s)}{1 + C_p s Z(s)} V_p(s).$$

When the piezoelectric transducer is shunted with a finite impedance Z, we may write

$$V_p(s) = G_{vv}(s) V_{in}(s) - G_{vv}(s) V_z(s). \tag{8}$$

By substituting (7) into the above equation, and simple algebra the transfer function relating $V_p(s)$ to $V_{in}(s)$, is found to be

$$\hat{G}_{vv}(s) \triangleq \frac{V_p(s)}{V_{in}(s)} = \frac{G_{vv}(s)}{1 + G_{vv}(s) K(s)} \tag{9}$$

where

$$K(s) = \frac{Z(s)}{Z(s) + \frac{1}{C_p s}}. \tag{10}$$

Also, it can be shown that,

$$\hat{G}_{yv}(x, s) \triangleq \frac{Y(x, s)}{V_{in}(s)} = \frac{G_{yv}(s)}{1 + G_{vv}(s) K(s)}. \tag{11}$$

From equations (9) - (11), it can be observed that shunt damping of piezoelectric transducer is in fact a feedback control problem. Therefore, it should be possible to use feedback control techniques to determine an appropriate impedance.

5. DEVELOPING THE NEGATIVE CAPACITANCE CONTROLLER

This section will develop the fundamental concept of the new broadband semi-active controller. Consider, the two following relationships, as in previous section,

$$\hat{G}_{vv}(s) = \frac{G_{vv}(s)}{1 + G_{vv}(s) K(s)} \tag{12}$$

with

$$K(s) = \frac{Z(s)}{Z(s) + \frac{1}{C_p s}} \tag{13}$$

where $G_{vv}(s)$ is the undamped response of the structure, C_p is the piezoelectric capacitance, and $Z(s)$ is the impedance of the shunt network. After straightforward manipulation, we obtain the following relationship for $\hat{G}_{vv}(s)$, i.e. the transfer function of a shunt damped mechanical structure, as

$$\hat{G}_{vv}(s) = \frac{G_{vv}(s) \left(C_p Z(s) s + 1\right)}{C_p Z(s) s \left(1 + G_{vv}(s)\right) + 1}. \tag{14}$$

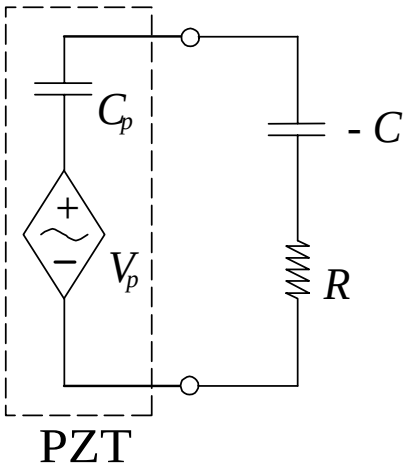

Figure 4. Negative capacitance controller with appropriate damping resistance.

The damped structural transfer function (14) can be minimized by equating the numerator to 0, i.e. by selecting $Z(s) = \frac{1}{-Cs}$, where $C = C_p$. This is not a realizable network as it creates an undamped electrical resonance. A compromise between damping performance and practicality (i.e. the node voltages and currents) can be achieved by introducing a series resistor R. The electrical model of the shunt piezoelectric with attached negative capacitor and resistor is shown in Figure 4. It should be noted that this control scheme is virtually immune to variations in structural dynamics since it is not tuned into specific frequencies, unlike passive shunt damping, networks that are extremely sensitive to variations in the resonant frequencies of the underlying structure.

If $Z(s)$ is chosen to be $-\frac{1}{Cs} + R$ then $Z(s)$ will have the following transfer function:

$$Z(s) = \frac{RCs - 1}{Cs}. \tag{15}$$

Substituting (15) in (13), $K(s)$ becomes

$$K(s) = \frac{s - \frac{1}{RC}}{s + \frac{1}{RC}\left(\frac{C}{C_p} - 1\right)}. \tag{16}$$

The shunt damped system will be stable if the capacitance of the controller $K(s)$, is greater than or equal to the capacitance of the piezoelectric patch i.e. if $C \geq C_p$[20] . In practice the equivalent electrical model of the piezoelectric element does not fully describe the piezoelectric dynamics, in particular the piezoelectric capacitance tends to be frequency dependent. To deal with this uncertainty C is chosen conservatively i.e. $C > C_p(f)\ \forall f \in \mathbb{R}$. For our case C was chosen to be $115nF$, since the nominated piezoelectric capacitance is $C_p = 105nF$.

6. OPTIMAL CHOICE FOR R

In order to find the appropriate value for resistor R, an optimization approach is proposed, such that the $\mathcal{H}_2$ norm of the combined system $\hat{G}_{yv}(x, s)$ is minimized for the first 5 structural modes. We have the following constrained optimization problem;

$$R^* = \arg \min_{\substack{s.t.\ \hat{\mathbf{A}}(R)^T\hat{\mathbf{P}}+\hat{\mathbf{P}}\hat{\mathbf{A}}(R)+\hat{\mathbf{B}}\hat{\mathbf{B}}^T=\mathbf{0} \\ R>0}} tr(\hat{\mathbf{C}}\hat{\mathbf{P}}\hat{\mathbf{C}}^T) \tag{17}$$

where $\hat{G}_{yv}(0.170, s) = \hat{\mathbf{C}}(s\mathbf{I} - \hat{\mathbf{A}}(R))^{-1}\hat{\mathbf{B}}$.

Using a line search algorithm, a local minimum was found at $R^* = 1309.9\Omega$. Figure 5, shows the $\mathcal{H}_2$ norm cost surface which contains a minima at R^*.

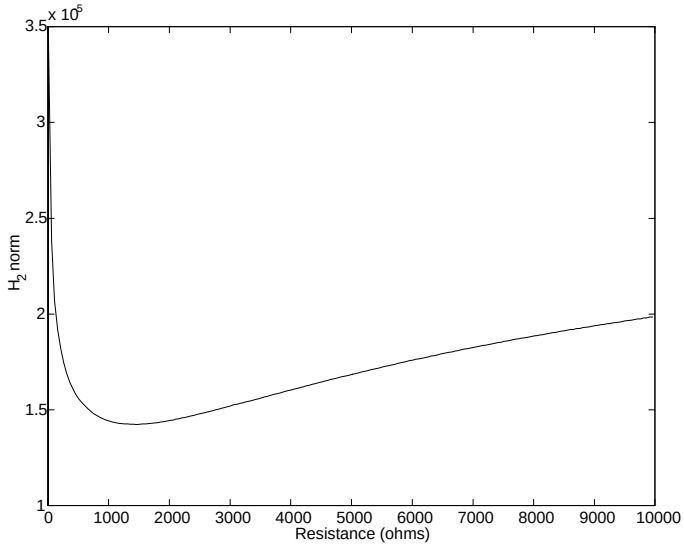

Figure 5. $G_{yv}(0.170, s)$ $\mathcal{H}_2$ norm plotted against resistance R (Ω), for 5 modes.

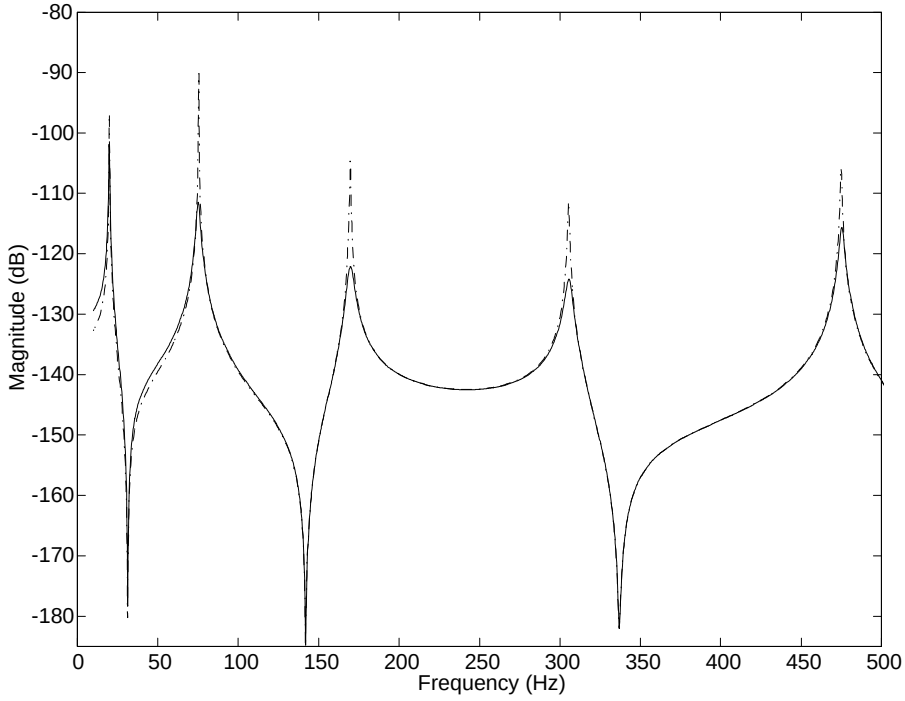

Figure 6. Simulated response: $|G_{yv}(0.170, s)|$ undamped $(\cdots)$ and $\left|\hat{G}_{yv}(0.170, s)\right|$ damped system (—).

7. SIMULATED RESULTS

Using $C = 115nF$ and $R^* = 1309.9\Omega$, simulations of $G_{yv}(0.170, s)$ and $\hat{G}_{yv}(0.170, s)$ show that the structural modes of the beam have been considerably dampened, as shown in Figure 6. From Figure 7, we can observe that the poles of the compound system have been pushed further to the left. By shifting the poles to the left we have added damping to the compound system, therefore effectively minimizing vibration of the structure. From Figure 7, we can foresee that the controller has a localized effect on the controlled poles.

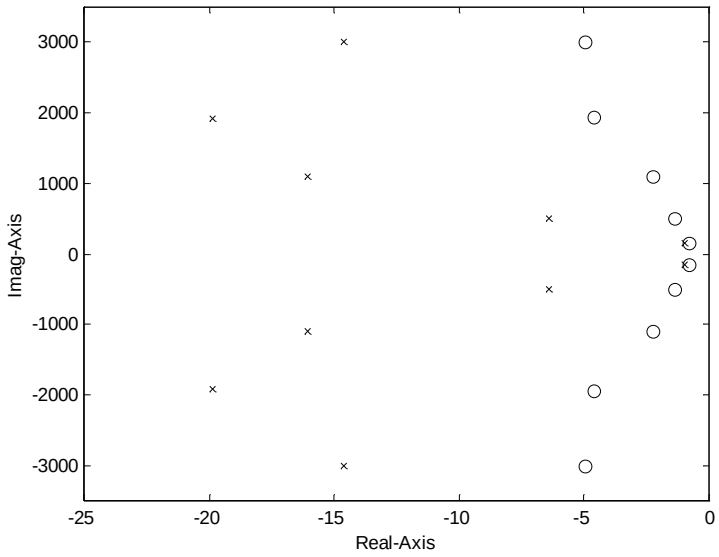

Figure 7. $G_{yv}(0.170, s)$ undamped poles (o) and $\hat{G}_{yv}(0.170, s)$ damped poles ($\times$).

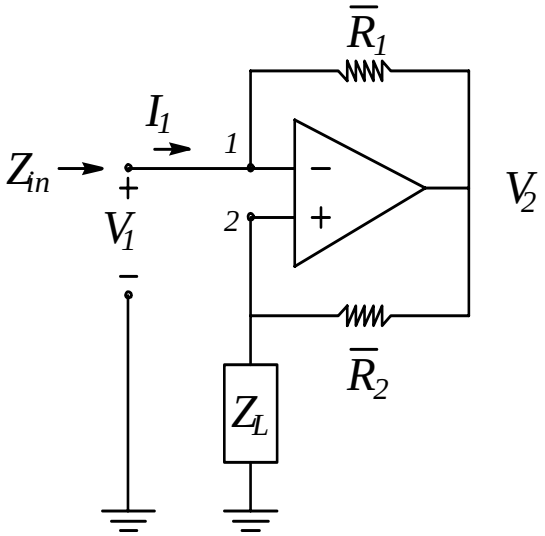

Figure 8. Example of a negative impedance converter.

8. EXPERIMENTAL RESULTS

8.1. Creating the Negative Capacitance

If our semi-active shunt circuit requires a negative capacitance element, how do we create such an element? To answer this question we begin with the following circuit given in Figure 8. If we use nodal analysis, at node 1 the Kirchhoff's current law implies

$$I_1 + \frac{V_2 - V_1}{\bar{R}_1} = 0 \tag{18}$$

and at node 2,

$$\frac{V_2 - V_1}{\bar{R}_2} + \frac{(0 - V_1)}{Z_L} = 0. \tag{19}$$

Eliminating V_2 from Equations (18) and (19) from these two equations, imply

$$-I_1\bar{R}_1 - \frac{V_1\bar{R}_2}{Z_L} = 0. \tag{20}$$

Solving for the ratio $\frac{I_1}{V_1}$, we obtain the following

$$Z_{in} = \frac{V_1}{I_1} = -\frac{\bar{R}_1}{\bar{R}_2}Z_L. \tag{21}$$

From these equations we can see that the circuit, shown in Figure 8, creates a negative impedance and also scales the value by the ratios of the resistors i.e. a transconductance gain. Thus if $Z_L = 1/Cs$, then $Z_{in} = -1/Cs$. The circuit shown is one of a general class of circuits known as a *negative impedance converter* (NIC).

We can now use this circuit for reducing the amplitudes of the resonant peaks of the structure. When considering this type of circuit we need to be aware that the impedance Z has become a semi-active shunt circuit. Therefore, stability issues need to be addressed when constructing the experimental circuit, e.g. bias currents due to operational amplifiers.

8.2. Test Example: Negative Capacitance Controller

A test circuit was constructed, as in Figure 9, with the appropriate components, tabulated in Table 2. Construction of the test circuit incorporated Burr-Brown OPA445 high voltage operational amplifiers. The frequency response was measured between the source voltage $\tilde{V}_{in}$, and the voltage across the semi-active controller $\tilde{V}_{out}$, as shown Figure 9. The simulated magnitude and phase response are plotted against the experimental responses, as illustrated in Figure 10. From experimental results we can see that the predicted theoretical results agree closely, therefore, verifying that the semi-active shunt controller is working correctly.

Circuit Component	**Value**
R	$10k\Omega$
R	$33M\Omega$
C≈C_p	$100nF$
C	$115nF$
R	$1.3k\Omega$

Table 2. Parameters of negative capacitance test circuit.

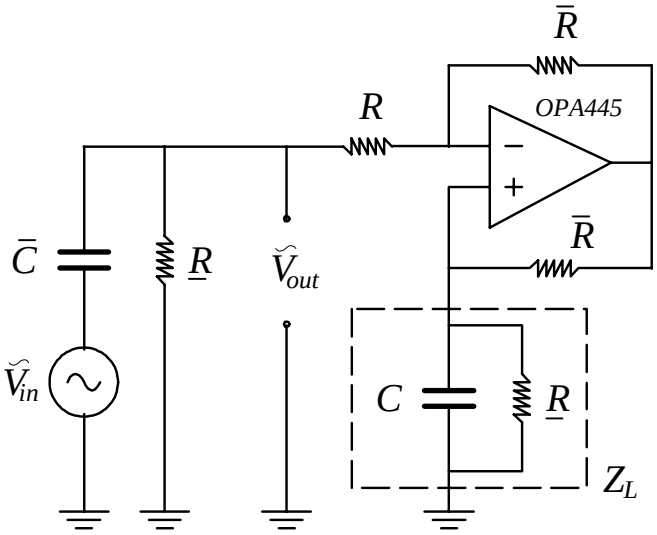

Figure 9. Test circuit with negative capacitance present.

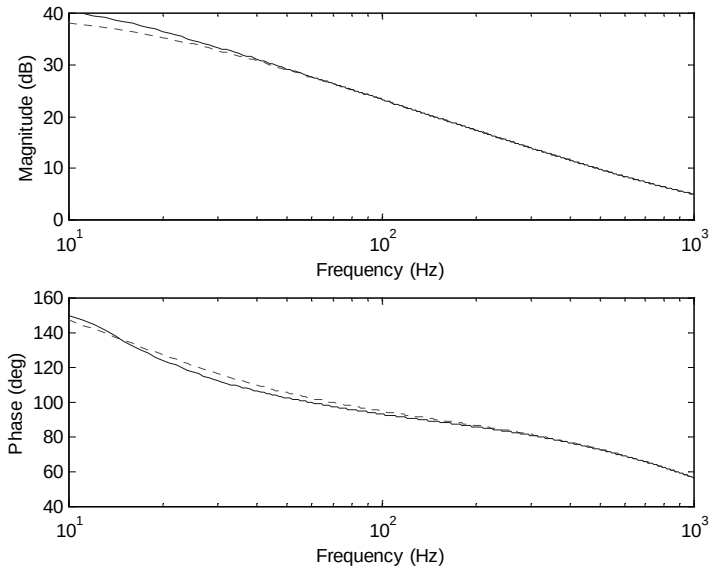

Figure 10. Frequency response $\tilde{V}_{out}(s)/\tilde{V}_{in}(s)$ of the test circuit: ideal $(\cdots)$ and experimental results (—).

8.3. Negative Capacitor Controller

Using the tested circuit from above, the semi-active negative controller is now applied to the piezoelectric laminated simply-supported beam. The displacement and actuator voltage frequency responses are measured using a Polytec Laser Scanning Vibrometer (PSV-300) and the Hewlett Packard function generator (33120A). A swept sine excitation is amplified then applied to the piezoelectric actuator.

The experimental resonant amplitudes for the $1st$, $2nd$, $3rd$, $4th$ and $5th$ modes were successfully reduced as shown in Figure 11. Resonant amplitudes were reduced by 6.1, 16.3, 15.2, 11.7 and $10.2dB$. From theoretical simulations the resonant amplitudes $1st$, $2nd$, $3rd$, $4th$ and $5th$ modes were 7.3, 22.4, 18.6, 13.4 and $11.8dB$ respectively. The analytical and experimental results show encouraging developments, as summarized in Table 3.

Negative Capacitance Amplitude Reduction		
Mode	Simulations (dB)	Experimental (dB)
1	7.3	6.1
2	22.4	16.3
3	18.6	15.2
4	13.4	11.7
5	11.8	10.2

Table 3. Amplitude reduction: simulations and experimental results.

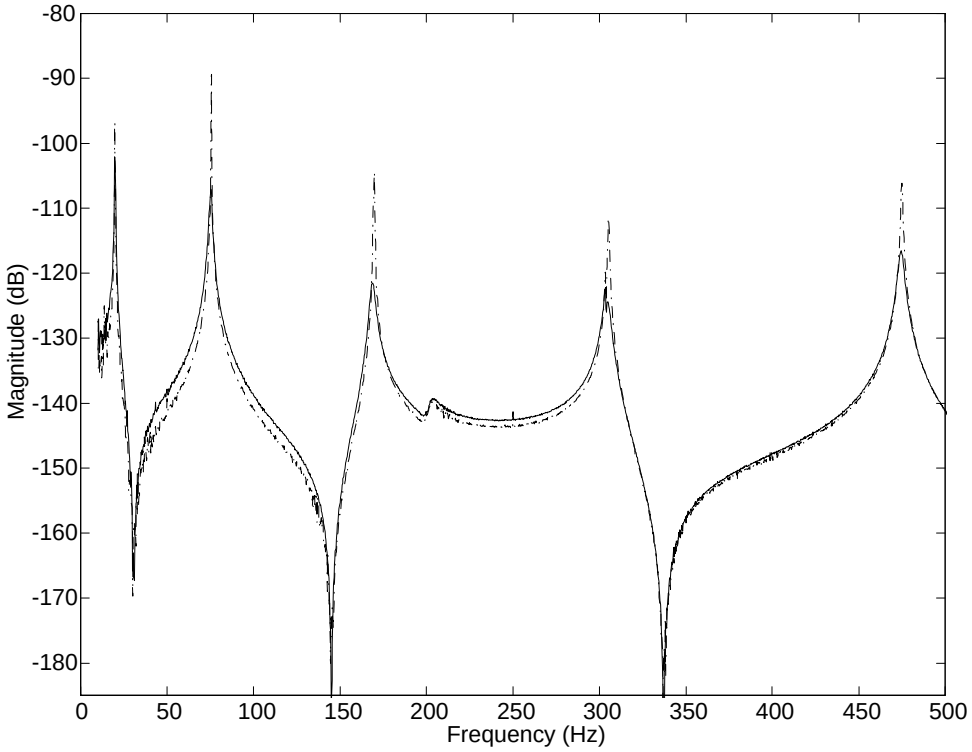

Figure 11. Experimental response: $|G_{yv}(0.170, s)|$ undamped $(\cdots)$ and $\left|\hat{G}_{yv}(0.170, s)\right|$ damped system (—).

9. CONCLUSION

The negative capacitor piezoelectric shunt circuit has been introduced as an alternate method of reducing structural vibrations. While achieving comparable performance, the negative capacitor has a number of advantages over current passive shunt damping systems: simplicity - it is non-model based (i.e. not dependent on resonant frequencies) and requires only a single operational amplifier for implementation; and robustness - the negative capacitor depends only on the dynamics of the piezoceramic device. A method has been presented for synthesizing a semi-active controller that alleviates some of the problems associated with passive control schemes with promising results. Resonant magnitudes have been reduced up to $16dB$ for multiple modes.

ACKNOWLEDGEMENTS

This research was supported by the Centre for Integrated Dynamics and Control (CIDAC) and the Australian Research Council (ARC).

REFERENCES

1. S. Y. Wu, "Piezoelectric shunts with parallel R-L circuit for smart structural damping and vibration control," In: *Proceedings SPIE: Smart Structures and Materials 1996: Passive Damping and Isolation* **2720**, pp. 259–269, March 1996.
2. S. Y. Wu, "Method for multiple mode shunt damping of structural vibration using a single PZT transducer," In: *Proceedings SPIE: Smart Structure and Materials 1998: Smart Structures and Intelligent System* **3327**, pp. 159–168, March 1998.
3. S. Y. Wu, "Multiple PZT transducer implemented with multiple-mode piezoelectric shunt for passive vibration damping," In: *Proceedings SPIE: Smart Structures and Materials 1999: Passive Damping and Isolation* **3672**, pp. 112–122, March 1999.
4. S. Y. Wu and A. S. Bicos, "Structure vibration damping experiments using improved piezoelectric shunts," In: *Proceedings SPIE: Smart Structures and Materials 1997: Passive Damping and Isolation* **3045**, pp. 40–50, March 1997.
5. W. W. Clark, "Semi-active vibration control with piezoelectric materials as variable-stiffness actuators," In: *Proceedings SPIE: Smart Structures and Materials 1999: Passive Damping and Isolation* **3672**, pp. 123–130, 1999.
6. C. L. Davis and G. A. Lesieutre, "An actively-tuned solid state piezoelectric vibration absorber," In: *Proceedings SPIE: Smart Structures and Materials 1998: Passive Damping and Isolation* **3327**, pp. 169–182, 1998.
7. C. L. Davis and G. A. Lesieutre, "An actively tuned solid-state vibration absorber using capacitance shunting of piezoelectric stiffness," *J. of Sound and Vibration* **232**(3), pp. 601–617, 2000.
8. C. Richard, D. Guyomar, D. Audigier and H. Bassaler, "Enhance semi-passive damping using continuous switching of a piezoelectric devices on an inductor.," In: *Proceedings SPIE: Smart Structures and Materials 2000: Damping and Isolation* **3989**, pp. 288–299, 2000.
9. C. Richard, D. Guyomar, D. Audigier and G. Ching, "Semi-passive damping using continuous switching of a piezoelectric device," In: *Proceedings SPIE: Smart Structures and Materials 1994: Passive Damping and Isolation* **3672**, pp. 104–111, 1999.
10. G. S. Agnes, "Active/passive piezoelectric vibration suppression," In: *Proceedings SPIE: Smart Structures and Materials 1994: Passive Damping* **2193**, pp. 24–34, 1994.
11. P. Bisegna, G. Caruso, D. Del Vescovo, S. Galeani and L. Menini, "Semi-active control of a thin piezoactuated structure," In: *Proceedings SPIE: Smart Structures and Materials 2000: Damping and Isolation* **3989**, pp. 300–311, 2000.
12. M. S. Tsai and K. W. Wang, "On the structural damping characteristics of active piezoelectric actuators with passive shunt," *J. of Sound and Vibration* **221**(1), pp. 1–22, 1999.
13. B. Clephas, *Adaptronics and Smart Structures - Basics, Material, Design, and Applications*, ch. 6.2, p. 106. Springer, 1999.
14. N. W. Hagood and E. F. Crawley, "Experimental investigations of passive enhancement of damping space structures," *J. of Guidance, Control and Dynamics* **14**(6), p. 1100, 1991.
15. N. W. Hagood and A. V. Flotow, "Damping of structure vibrations with piezoelectric materials and passive electrical networks," *J. of Sound and Vibration* **14**(2), p. 243, 1991.
16. C. R. Fuller, S. J. Elliott and P. A. Nelson, *Active Control of Vibration*, Academic Press, 1996.
17. S. O. R. Moheimani, "Experimental verification of the correction transfer function of a piezoelectric laminated beam," *IEEE Transactions on Control Systems Technology* **8**, pp. 660–666, July 2000.
18. L. Meirovitch, *Elements of Vibration Analysis*, McGraw-Hill, Sydney, 2nd ed., 1996.
19. N. W. Hagood, W. H. Chung and A. V. Flowtow, "Modelling of piezoelectric actuator dynamics for active structural control," *J. of Intelligent Material Systems and Structures* **1**, pp. 327–353, July 1990.
20. S. Behrens and A. J. Fleming, "Negative capacitor for multiple mode shunt damping of a piezoelectric laminate beam," Technical Report EE0045, Electrical and Computer Engineering, University of Newcastle, October 2000.